Vicinage effects in energy loss and electron emission during grazing scattering of heavy molecular ions from a solid surface

Yuan-Hong Song* and You-Nian Wang
The State Key Laboratory of Materials Modification by Laser, Electron, and Ion Beams, Department of Physics, Dalian University of Technology, Dalian 116024, People's Republic of China

Z. L. Mišković
Department of Applied Mathematics, University of Waterloo, Waterloo, Ontario, Canada N2L 3G1
(Received 29 March 2005; published 20 July 2005)

Vicinage effects in the energy loss and the electron emission spectra are studied in the presence of Coulomb explosion of swift, heavy molecular ions, during their grazing scattering from a solid surface. The dynamic response of the surface is treated by means of the dielectric theory within the specular reflection model using the plasmon pole approximation for the bulk dielectric function, whereas the angle-resolved energy spectra of the electrons emitted from the surface are obtained on the basis of the first-order, time-dependent perturbation theory. The evolution of the charge states of the constituent ions in the molecule during scattering is described by a nonequilibrium extension of the Brandt-Kitagawa model. The molecule scattering trajectories and the corresponding Coulomb explosion dynamics are evaluated for the cases of the internuclear axis being either aligned in the beam direction or randomly oriented in the directions parallel to the surface. Our calculations show that the vicinage effect in the energy loss is generally weaker for heavy molecules than for light molecules. In addition, there is clear evidence of the negative vicinage effect in both the energy loss and the energy spectra of the emitted electrons for molecular ions at lower speeds and with the axis aligned in the direction of motion.

DOI: 10.1103/PhysRevA.72.012903 PACS number(s): 34.50.Bw, 34.50.Dy, 61.80.−x

I. INTRODUCTION

Interactions of swift cluster and molecular ions with solids have been studied with increasing interest over the past decades in the context of possible applications in plasma physics and materials research. In comparison with single-ion beams, molecular- and cluster-ion beams interact with the medium in a coherent way, providing a host of new phenomena, commonly referred to as the vicinage effect, occurring in the energy loss, screening, charge states, and the dynamical evolution of the projectile constituents.

Scattering of fast molecular ions from solid surfaces under grazing angles of incidence is expected to present new manifestations of the vicinage effect. One of the most typical processes is Coulomb explosion of the projectile: when a swift molecular ion impinges on a solid, it loses its binding valence electrons, and the resulting ionic fragments begin to recede from each another under the influence of Coulomb repulsion, and eventually separate after several femtoseconds. Experimental observation of Coulomb explosion has been first reported by Susuki *et al.* [1] for MeV H_2^+ and HeH^+ grazing scattering from a clean surface of SnTe. Similar experiments were conducted shortly thereafter by Winter [2], in which clearly resolved Coulomb explosion patterns in the energy spectra of the dissociated fragments were obtained for H_2^+ scattering from Si and W surfaces. Numerical simulations, performed by Susuki *et al.* [3,4] in conjunction with their experimental measurements, suggest that almost all molecular ions dissociate during grazing scattering and that pronounced alignment of the internuclear axis takes place parallel to the surface plane.

Vicinage effect is also manifested in the energy loss of molecular ions, which generally differs from the incoherent sum of the energy losses of individual ions scattered from the surface under identical conditions, due to interferences in the electronic excitations of the surface coming from the spatial correlation between the constituent ions. Brandt *et al.* [5] were the first to demonstrate experimentally the existence of the vicinage effects in energy losses of molecular hydrogen ions traversing carbon foils. This pioneering work was followed by numerous studies of the deposition of energy by swift molecules and clusters in solids, which were recently reviewed [6,7]. Regarding the energy loss of light molecular ions on solid surfaces, Susuki [8] measured experimentally the energy losses of MeV H_2^+ ions after grazing scattering from a SnTe surface and observed a positive vicinage effect. This effect was confirmed by theoretical calculations of the energy losses due to collective excitations of the electron gas on the surface, based on a local dielectric function, both with [9] and without [8] the effects of damping of these excitations. However, negative vicinage effects were reported for energy losses of heavier molecular ions, such as N_2^+ and O_2^+, in thin solid foils [10]. Such projectiles are not completely stripped of their electrons at intermediate speeds, especially in the initial stages of the interaction, which should affect the dynamics of Coulomb explosion and the rate of energy deposition in the target in comparison with hydrogen molecular ions. In particular, the vicinage effect in the constituent-ion charges for fast H_2^+ projectiles moving

*Email address: songyh@dlut.edu.cn

through a carbon foil was shown to slow down the Coulomb explosion and reduce the energy loss in comparison to the penetration of individual nitrogen ions at the same speed [11,12]. It is therefore expected that ion charge states in heavier molecular projectiles may also play an important role in the vicinage effects for grazing scattering from solid surfaces.

In the course of grazing scattering of single-ion beams on solid surfaces, the angular and energy distributions of the emitted electrons may provide important information on the state of the surface owing to the long time of interaction. The so-called kinetic electron emission (KEE), in which the electron excitations are induced by the transfer of kinetic energy from the incident particles, is of particular interest. For example, analyzing the maximum of energy that can be transferred to the electron gas can help determine the threshold velocity for the kinetic emission [13], as recently shown both theoretically and experimentally [14,15]. For the kinetic mechanism of electron emission, the excitations of the valence-band electrons in the near-surface region are important at large ejection angles, with two processes involved: the collective excitations giving rise to the surface plasmon field, and the single-particle excitations via binary collisions with the projectile. Several theoretical investigations of KEE during single-ion grazing surface scattering were reported recently, using both the dielectric formalism [16,17] and quantum-mechanical models [18], which were based, respectively, on the specular-reflection model (SRM) [19] or the modified specular-reflection (MSR) [20], and a simple Yukawa model for the surface induced potential. As is generally believed, the kinetic electron emission is closely related to the projectile energy loss. Thus the energy spectra of kinetic electron emission for molecular ions, grazingly scattered from a solid surface, may exhibit vicinage effects similar to the vicinage effects in stopping power. In that context, the vicinage effect in the total secondary electron emission yield from SnTe crystal has been studied under the keV hydrogen cluster incidence [21]. However, as far as we know, there are no reports on investigations of vicinage effects in the energy and angular distributions of electron emission from solid surfaces, induced by glancing-angle incidence of heavier molecular ions or clusters.

Therefore the main purpose of the present work is to study in detail the vicinage effects in the energy loss and the energy spectra of electron emission induced by fast, heavy molecular ions grazingly scattered from a solid surface. In accordance with our previous work [19,22], the present theoretical description is based on the dielectric response theory within SRM, allowing appropriate descriptions of the scattering trajectory, stopping power, and the energy loss of fast heavy diatomic molecular ions, taking into account Coulomb explosion and the evolution of charge states of the constituent ions. The differential electron emission probabilities for diatomic molecular ions will be calculated along the whole scattering trajectory by means of the first-order quantum perturbation theory. The surface induced potential will be obtained in Sec. II, the dynamics of Coulomb explosion will be studied in Sec. III, the molecular energy loss will be calculated in Sec. IV, and the electron emission spectra will be evaluated in Sec. V. Concluding remarks will be given in Sec. VI. Unless otherwise indicated, atomic units (a.u.), where $m_e=\hbar=e=1$, will be used throughout this paper.

II. SURFACE INDUCED POTENTIAL

When a diatomic ion moves near a solid surface with velocity $\mathbf{v}$, the initial directions of the molecular axis are randomly distributed with respect to the beam direction. However, experimental results [3] indicate that the internuclear vector tends to align itself along the surface due to the repulsive forces of the surface atoms and the surface wake potential coming from the dynamic response of surface electrons to the incident charged fragments. On the other hand, the dynamically screened interaction force between the two charges is asymmetric in such a way that the parallel component of this force is much stronger than the perpendicular one, resulting in an alignment of the molecular axis in the beam direction after a long enough time [24]. These alignment effects definitely influence the stopping power and Coulomb explosion patterns, as well as the electron emission, during grazing scattering of molecular ions. From the above reasons, two types of orientations will be considered in this work, with the internuclear axis either randomly oriented in a plane parallel to the surface or aligned in the direction of the projectile motion.

For an incident homonuclear diatomic molecular ion with the internuclear axis parallel to the surface plane, a Cartesian coordinate system is placed in the scattering plane with the z axis perpendicular to the surface and the x axis along the direction of motion. The origin $(x=0,z=0)$ is placed at a target-atom nucleus in the first atomic plane, such that the region $z'=z-r_d<0$ is occupied by the electron gas of the bulk of the solid, where r_d is the average atomic radius of the target. The notations $\mathbf{r}=(\mathbf{R},z)$, $\mathbf{k}=(\mathbf{Q},k_z)$, and $\mathbf{v}=(\mathbf{v}_\parallel,v_z)$ will be used, where $\mathbf{R}$, $\mathbf{Q}$, and $\mathbf{v}_\parallel$ represent components parallel to the surface. Given that the angle of incidence θ is of the order of milliradian, we may assume that the molecular ion velocity $\mathbf{v}\approx\mathbf{v}_\parallel$.

Similar to our previous work [19], the charge density of the molecular ion can be expressed as

$$\rho_{ext}(\mathbf{r},t)=[Z_1\delta(\mathbf{R}-\mathbf{R}_1-\mathbf{v}t)-\sigma_n(\mathbf{R}-\mathbf{R}_1-\mathbf{v}t)]\delta(z-z_0)+[Z_1\delta(\mathbf{R}-\mathbf{R}_2-\mathbf{v}t)-\sigma_n(\mathbf{R}-\mathbf{R}_2-\mathbf{v}t)]\delta(z-z_0), \quad (1)$$

where Z_1 is the atomic number of the projectile constituents, while $(\mathbf{R}_1,z_0)$ and $(\mathbf{R}_2,z_0)$ are the positions of the leading and the trailing ions, respectively. Here, $\sigma_n(\mathbf{R})$ is a two-dimensional projection of the bound-electron distribution, previously developed in a modification of the Brandt-Kitagawa (BK) statistical model [23] for the case of partially stripped ions moving through nonhomogeneous electron density at a solid surface. This assumption about the two-dimensional electron distribution might be feasible while considering the very small incidence angles and allows us to remain the boundary continuities during the calculation.

According to the surface dielectric theory within SRM, the total potential in the presence of a diatomic projectile can be written in the form which includes the contributions from

two individual ions, $\phi(\mathbf{r},t)=\phi_1(\mathbf{r},t)+\phi_2(\mathbf{r},t)$, where the potential from the ith ion is given by [19,22]

$$\phi_i(\mathbf{r},t)=\frac{1}{2\pi}\int\frac{d\mathbf{Q}}{Q}\tilde{\sigma}(Q)G(Q,\omega,z',z_0')e^{i\mathbf{Q}\cdot(\mathbf{R}-\mathbf{R}_i-\mathbf{v}t)}\quad(i=1,2). \tag{2}$$

Here $G(Q,\omega,z',z_0')$ is an interaction function, $\tilde{\sigma}(Q)=Z_1[q(z_0)+(Q\Lambda)^2]/[1+(Q\Lambda)^2]$ with Λ being the screening length [23], $q(z_0)=1-N_n(z_0)/Z_1$ the ionization degree, and $N_n(z_0)$ the number of electrons bound to the ion at distance z_0. The induced potential can be similarly decomposed, with the contribution from the ith ion being given by Eq. (2) in which $G(Q,\omega,z',z_0')$ is to be replaced by $F(Q,\omega,z',z_0')=G(Q,\omega,z',z_0')-e^{-Q|z'-z_0'|}$, with $e^{-Q|z'-z_0'|}$ corresponding to bare Coulomb potential, as discussed in detail elsewhere [19,21].

In order to calculate the interaction function $G(Q,\omega,z',z_0')$, one has to specify the local surface dielectric function $\epsilon_s(Q,\omega,z')$. In this work, we adopt the plasmon pole approximation (PPA) for the bulk dielectric function, $\epsilon(k,\omega)=1+\omega_p^2/[k^4/4+\beta^2k^2-\omega(\omega+i\gamma)]$, which describes both the collective and the single-electron excitations. Here $\omega_p=(4\pi n_0)^{1/2}$ is the bulk plasmon frequency, $\beta=\sqrt{3/5}v_F$ is the speed of propagation of the density disturbances, $v_F=(3\pi^2n_0)^{1/3}$ is Fermi speed, and n_0 is the bulk electron-gas density. In order to include the plasmon dispersion from the perpendicular component k_z of the wave number $\mathbf{k}$ into the surface dielectric function, one has to perform a contour integration involving three poles in the upper-half complex plane, at $u_{1,2}=i(Q^2+2\varsigma_\pm)^{1/2}$ and $u_3=iQ$, giving the following analytical expression for the surface dielectric function [25]:

$$\epsilon_s(Q,\omega,z')=\frac{\omega(\omega+i\gamma)}{\Omega}e^{-Q|z'|}+\frac{\omega_p^2Q}{\varsigma_+-\varsigma_-}\times\left[\frac{e^{-(Q^2+2\varsigma_-)^{1/2}|z'|}}{(Q^2+2\varsigma_-)^{1/2}\varsigma_-}-\frac{e^{-(Q^2+2\varsigma_+)^{1/2}|z'|}}{(Q^2+2\varsigma_+)^{1/2}\varsigma_+}\right], \tag{3}$$

where $\Omega=\omega(\omega+i\gamma)-\omega_p^2$ and $\varsigma_\pm=\beta^2\pm\sqrt{\beta^4+\Omega}$.

Another physical process that has to be taken into account in the present study concerns the evolution of charge states of the two constituent ions in the course of scattering. To simplify the simulation, we neglect the vicinage effects in ion charge states and assume that the charge states of the constituent ions are identical to those of individual ions scattered under identical conditions. For grazing scattering of fast ions from a solid surface, efficient charge exchange processes occur within the electron gas. Consequently, we adopt the picture where the ion charge state remains unchanged when the ion is outside the electron gas, $z_0>r_d$. The transient charge state effect is described by a model [26] in which the average number of electrons bound to each constituent ion can be defined as a function of the time elapsed from the instant when the molecular ion entered the electron gas. For a projectile at speed v, we therefore express the number of bound electrons at each ion in terms of the path length s_b traveled by the projectile through the electron gas, $z_0<r_d$, as follows:

$$N_n(s_b)=N_\infty-(N_\infty-N_0)\exp(-n_0s_b\Sigma), \tag{4}$$

where N_∞ and N_0 are, respectively, the number of electrons in equilibrium inside the solid and the initial number at the entrance. N_∞ is obtained from an empirical model [27] dependent on the speed v, which shows remarkably good agreement with experimental values for heavy ions in solids, whereas we assume $N_0=Z_1-0.5$ for an initially singly charged diatomic molecule. In Eq. (4), Σ is the ionization cross section.

III. DYNAMICS OF COULOMB EXPLOSION

When a diatomic molecular ion approaches a solid surface, in addition to the forces acting on individual constituent ions, coming from collective excitations of the electron gas and from the repulsive potentials of surface atoms, there also exist the bare Coulomb repulsion force and the interparticle wake interaction. These interionic forces give rise to a wake-modulated Coulomb explosion, which begins as soon as the projectile enters the electron gas and the charge exchange begins. According to the procedure outlined in [9], we obtain the trajectory of the molecule center of mass (c.m.) in the laboratory frame as follows:

$$\frac{dz_0}{dx_0}=\mp\theta\sqrt{1-2\frac{U_p(z_0)+U_s(z_0)+U_w(z_0,\mathbf{R}_0)}{E\theta^2}}, \tag{5}$$

while the equations of motion for the internuclear vector $\mathbf{R}_0=\mathbf{R}_1-\mathbf{R}_2$ and the relative velocity $\mathbf{u}$ are given by

$$\frac{d\mathbf{R}_0}{dx_0}=\frac{\mathbf{u}}{v},$$

$$\frac{d\mathbf{u}}{dx_0}=\frac{1}{vm}(\mathbf{F}^{(c)}+\mathbf{F}^{(w)}), \tag{6}$$

where (x_0,z_0) and $E=M_cv^2/2$ are the position and the initial kinetic energy of the molecule c.m., $M_c=2m$ is the mass of the molecule, and $U_p(z_0)$ and $U_s(z_0)$ are, respectively, the surface continuum potential and the surface image potential for individual ions [19]. Note that $\mp$ in Eq. (5) correspond to the incoming and the outgoing trajectories. The dynamical image interaction potential, $U_w(z_0,\mathbf{R}_0)=(U_w^{12}+U_w^{21})/2$, between the constituent ions is given by

$$U_w(z_0,\mathbf{R}_0)=\frac{1}{4\pi}\int\frac{d\mathbf{Q}}{Q}[\tilde{\sigma}(Q)]^2\times\mathrm{Re}[F(Q,\omega,z_0',z_0')]\cos(\mathbf{Q}\cdot\mathbf{R}_0), \tag{7}$$

where $\omega\equiv\mathbf{Q}\cdot\mathbf{v}$. The Coulomb force $\mathbf{F}^{(c)}=2\mathbf{F}_{12}^{(c)}$ between these ions is given by

$$\mathbf{F}_{12}^{(c)}=Z_1^2\left\{\frac{1}{R_0^2}+\int QdQ\left[\frac{2(q-1)}{1+(Q\Lambda)^2}+\left(\frac{(q-1)}{1+(Q\Lambda)^2}\right)^2\right]J_1(QR_0)\right\}\mathbf{e}_{\mathbf{R}_0}, \tag{8}$$

where $J_1(QR_0)$ is a Bessel function of the first order and $\mathbf{e}_{\mathbf{R}_0}$

is the unit vector in the direction of $\mathbf{R}_0$, whereas the oscillatory dynamic-wake interaction force between the ions, $\mathbf{F}^{(w)} = \mathbf{F}_{12}^{(w)} - \mathbf{F}_{21}^{(w)}$, is given by

$$\mathbf{F}^{(w)} = \frac{1}{\pi} \int \frac{\mathbf{Q} d\mathbf{Q}}{Q} [\tilde{\sigma}(Q)]^2 \, \mathrm{Re}[F(Q, \omega, z_0', z_0')] \sin(\mathbf{Q} \cdot \mathbf{R}_0). \tag{9}$$

As the molecular ion begins dissociating, Eqs. (5) and (6) will be solved simultaneously to obtain the scattering trajectory and the Coulomb explosion dynamics.

In the case when the internuclear axis is randomly oriented, but parallel with the solid surface, one can average Eqs. (7) and (9) over the directions of $\mathbf{R}_0$ to obtain the dynamical image interaction potential

$$\bar{U}_w(z_0, \mathbf{R}_0) = \frac{1}{4\pi} \int \frac{d\mathbf{Q}}{Q} [\tilde{\sigma}(Q)]^2 \, \mathrm{Re}[F(Q, \omega, z_0', z_0')] J_0(QR_0), \tag{10}$$

and the interaction force

$$\bar{\mathbf{F}}^{(w)} = \frac{1}{\pi} \int \frac{d\mathbf{Q}}{Q} [\tilde{\sigma}(Q)]^2 \, \mathrm{Re}[F(Q, \omega, z_0', z_0')] \mathbf{Q} J_1(QR_0), \tag{11}$$

where $J_0(QR_0)$ is the zeroth order Bessel function. In the case when the axis is aligned in the direction of motion of the molecule c.m., we suppose that the internuclear vector $\mathbf{R}_0$ and the velocity $\mathbf{v}$ are directed along the x axis, so that in Eqs. (7) and (9) one has explicitly $\mathbf{Q} \cdot \mathbf{R}_0 = QR_0 \cos\varphi$ and $\omega = \mathbf{Q} \cdot \mathbf{v} = Qv \cos\varphi$, where φ is polar angle in the $\mathbf{Q}$ plane. These specifications for the two cases of the internuclear axis orientations will be also used in the following calculations of the energy loss and the electron emission.

For the illustrative purposes, we are going to study grazing scattering of N_2^+ ions from a C surface, for which $n_0 = 4 \times 10^{23}$ cm^{-3}, $\Sigma \approx 10^{-17}$ cm^2 [26], $v_F = 1.17$, $\gamma = 0.3675$, and $r_d = 2.418$, while we take $R_0 = 2.117$ for the initial internuclear distance in the nitrogen molecular ion N_2^+. The evolution of the internuclear separation during Coulomb explosion of N_2^+ on a C surface, with the molecule speed $v = 3$ and the incident angle $\theta = 3$ mrad, is shown in Fig. 1 where we compare the cases of molecules with randomly oriented and aligned molecular axes, as well as the case of scattering without wake forces. One can easily see that the Coulomb explosion is more efficient in the absence of wake forces, especially in the outgoing leg of the scattering trajectory. It also appears that, in the case of an aligned axis, the ions penetrate deeper in the electron gas and the Coulomb explosion proceeds faster in close vicinity of the surface. In the outgoing part of the trajectory, owing to the oscillatory nature of the wake force, the two ions become more attracted to each other when the axis is aligned than in the case with a randomly oriented axis, resulting in a slower explosion.

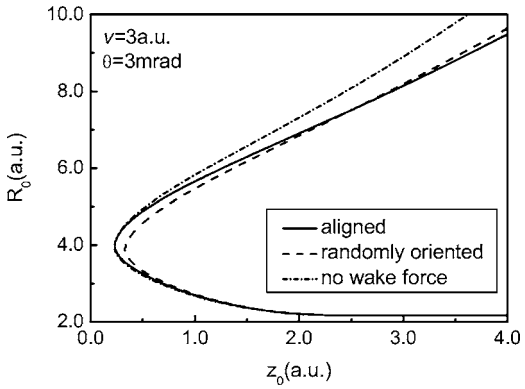

FIG. 1. Internuclear separation R_0 vs distance from the first atomic layer z_0, during grazing scattering of N_2^+ from a C surface at speed $v = 3$ a.u. with incident angle $\theta = 3$ mrad. Comparisons of Coulomb explosions are shown for the cases of: molecular axis aligned in the direction of motion (solid line), molecular axis randomly oriented in a plane parallel to the surface (dotted line), and grazing scattering without wake forces (dot-and-dash line).

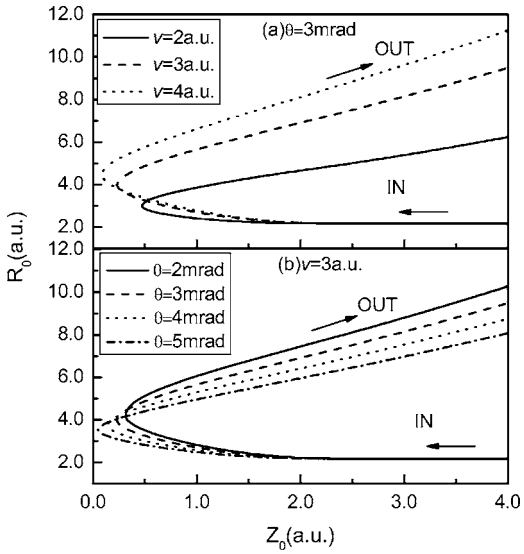

FIG. 2. Internuclear separation R_0 vs distance from the first atomic layer z_0, during grazing scattering of N_2^+ from a C surface with the molecular axis aligned in the direction of motion, for (a) several incident speeds and fixed incident angle, and for (b) several incident angles and fixed incident speed.

The dependences of Coulomb explosion on the incident speed and the incident angle are shown in Fig. 2, with the internuclear vector aligned in the beam direction. Comparing the trajectories, it is obvious that, at higher speeds, the ions penetrate deeper into the electron gas and dissociate more quickly. However, as the incident angle increases, the Coulomb explosion becomes weaker, although the ions approach the surface closer. This is due to shorter interaction times with the surface for larger incident angles.

IV. STOPPING POWER AND ENERGY LOSS

Based on the expression for induced potential, one can obtain the position-dependent stopping power of the molecular ion as follows:

$$S_{mol}(z_0, R_0) = 2S_e(z_0) + S_v(z_0, R_0), \tag{12}$$

where $S_e(z_0)$ is the stopping power of an individual ion,

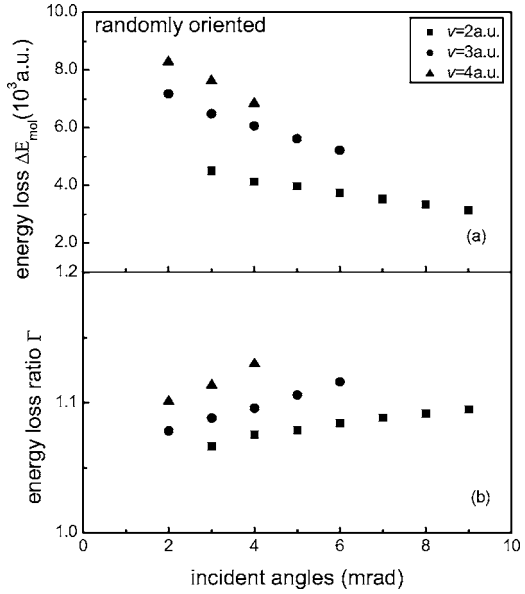

FIG. 3. The dependences of (a) the total energy loss and (b) the energy loss ratio on the incident angle for N_2^+ ions grazingly scattered from a C surface, at speeds $v=2$, 3, and 4 a.u., for the molecular axis randomly oriented in a plane parallel to the surface.

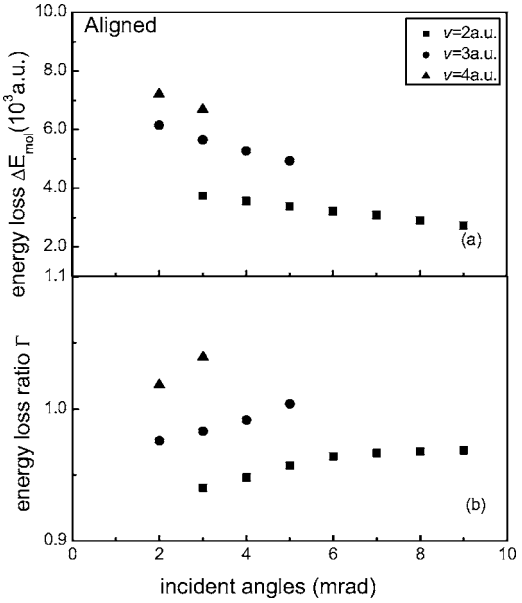

FIG. 4. The dependences of (a) the total energy loss and (b) the energy loss ratio on the incident angle for N_2^+ ions grazingly scattered from a C surface, at speeds $v=2$, 3, and 4 a.u., for the molecular axis aligned with the beam direction.

$$S_e(z_0) = \frac{1}{2\pi v}\int \frac{d\mathbf{Q}}{Q}[\tilde{\sigma}(Q)]^2(-\mathbf{Q}\cdot\mathbf{v})\mathrm{Im}[F(Q,\omega,z_0',z_0')], \tag{13}$$

while $S_v(z_0,R_0)$ is the interference term due to the vicinage effect which depends on the relative position of the two ions,

$$S_v(z_0,R_0) = \frac{1}{\pi v}\int \frac{d\mathbf{Q}}{Q}[\tilde{\sigma}(Q)]^2(-\mathbf{Q}\cdot\mathbf{v}) \times \mathrm{Im}[F(Q,\omega,z_0',z_0')]\cos(\mathbf{Q}\cdot\mathbf{R}_0). \tag{14}$$

As before, the average vicinage stopping power for a randomly oriented molecular axis is given by

$$\bar{S}_v(z_0,R_0) = \frac{1}{\pi v}\int \frac{d\mathbf{Q}}{Q}[\tilde{\sigma}(Q)]^2(-\mathbf{Q}\cdot\mathbf{v}) \times \mathrm{Im}[F(Q,\omega,z_0',z_0')]J_0(QR_0). \tag{15}$$

Finally, the total energy loss of the molecular ion can be calculated by integrating the stopping power along the whole c.m. scattering trajectory,

$$\Delta E_{mol} = \int_{-\infty}^{\infty} S_{mol}(z_0,R_0)ds, \tag{16}$$

where $ds=\sqrt{dx_0^2+dz_0^2}$. Moreover, the energy loss ratio $\Gamma \equiv \Delta E_{mol}/(2\Delta E)$ can be considered a measure of the vicinage effect, with ΔE being the energy loss of a single ion under identical scattering conditions.

The dependences of the energy loss ΔE_{mol} and the energy loss ratio Γ on incident angle are shown in Fig. 3 for several speeds, when the internuclear axis is randomly oriented. One can see in this figure that the energy loss ratio increases, whereas the absolute energy loss decreases, with increasing incident angles, which is readily explained by shorter interaction times with electron gas at higher incident angles, and also in view of the fact that we neglect the contribution from the inner shell excitations in this work. On the other hand, the rates of changes of the quantities shown in Fig. 3 increase with incident speed of the molecular ion. This can be rationalized by the fact that more electrons are stripped off at higher ion speeds, leading to stronger interactions with the electron gas, as well as stronger interaction between the constituent ions. For this same reason the two ions dissociate faster at higher molecular speeds, as shown in Fig. 2(a). It can be also concluded that the energy loss ratios for N_2^+ ions remain around one, which is smaller than in the case of grazing scattering of H_2^+ [9]. Thus, for the molecules made of heavier atoms, owing to partial stripping of their valence electrons and to the resulting weakening of the interference effects, less enhancement in the energy loss ratio is expected than for light molecules.

In the case of the axis aligned in the direction of motion, the dependences of the total energy loss and the energy loss ratio on the incident angle are shown in Fig. 4 for the same set of parameters as in Fig. 3. Both the absolute energy loss and the energy loss ratio are smaller in this case than those for a randomly oriented molecular axis. Moreover, comparison of the parts (b) in Figs. 3 and 4 shows that a negative vicinage effect occurs in the case of aligned molecular axis, with the energy loss ratio being less than one for speeds $v=2$ and $v=3$, suggesting that the total energy losses of the molecular ion are smaller than the losses of two separated ions. This appears to be consistent with the discussion in [6,7], where more pronounced negative interferences have been predicted in the vicinage effect at lower projectile speeds and for the aligned internuclear vector when the molecular ions move in solids.

V. ELECTRON EMISSION

Considering the close relationship between the stopping power and the electron emission, one expects that the interference in the electronic excitations of the surface induced by a molecular ion may also exert strong vicinage effects in the electron emission. Treating the solid in jellium approximation, the electrons can be considered quasifree within the solid and confined in the $z'<0$ region by a step potential $V=V_0\Theta(-z')$, where $V_0=E_F+\Phi$, with E_F being Fermi energy and Φ work function. On using the first-order, time-dependent perturbation theory involving the electron states at the step potential barrier, one obtains the expression for transition amplitude, based on the approximate expression for the perturbed wave function in terms of the screened potential [28,29], viz.,

$$\mathbf{M}_{\varkappa\leftarrow\mathbf{l}_0}=m_{\varkappa\leftarrow\mathbf{l}_0}\delta(\omega-\mathbf{Q}\cdot\mathbf{v})(e^{-i\mathbf{Q}\cdot\mathbf{R}_1}+e^{-i\mathbf{Q}\cdot\mathbf{R}_2}), \quad (17)$$

where $\mathbf{Q}=\mathbf{l}_\parallel^1-\mathbf{l}_\parallel^0$, with $\mathbf{l}_0=(\mathbf{l}_\parallel^0,l_z^0)$ and $\mathbf{l}_1=(\mathbf{l}_\parallel^1,l_z)$ being, respectively, the initial and the final momenta of the electron, while $\varkappa=(\mathbf{l}_\parallel^1,\varkappa_z)$ is the momentum of the electron in vacuum. The detailed expression for $m_{\varkappa\leftarrow\mathbf{l}_0}$ is given in Ref. [17], including the expression $\tilde{\sigma}(Q)$ which denotes the effect produced by projectile ionization. The factor $(e^{-i\mathbf{Q}\cdot\mathbf{R}_1}+e^{-i\mathbf{Q}\cdot\mathbf{R}_2})$ in Eq. (17) introduces interference effects due to correlated excitations of the surface electrons by the constituent ions placed at the positions $(\mathbf{R}_1,z_0)$ and $(\mathbf{R}_2,z_0)$. Considering the transport of excited electrons towards the surface, the effect of inelastic collisions is included approximately through an exponential factor $e^{\mu z}$, where μ is proportional to the inverse of the electron mean free path in the bulk of the target. The triple differential probability for electron emission can be obtained as a function of the distance z_0 as follows:

$$\frac{d^3P}{d\varkappa}=8\pi\int d\mathbf{l}_\parallel^0\Theta(E_F-\varepsilon_0)\Theta(l_1^2-(l_\parallel^0)^2-\mathbf{Q}\cdot\mathbf{v})|m_{\varkappa\leftarrow\mathbf{l}_0}|^2\times[1+\cos\mathbf{Q}\cdot\mathbf{R}_0], \quad (18)$$

where ε_0 is the initial energy of the electron, while the two step functions Θ define the initial and the emitted states of electrons.

Considering the grazing scattering geometry for molecular ions, the total electron emission distribution can be obtained by integrating the above expression along the molecule c.m. trajectory. Noting that the scattering trajectory is not symmetrical due to the effects of Coulomb explosion and the charge state evolution, we define the initial position of the molecular ion to be at the entrance to the bulk electron gas, $x'=0$, and obtain the integrated electron emission probability, $W_{mol}=2W_s+W_v$, where W_s is the electron emission probability induced by an isolated ion,

$$W_s=\frac{4\pi}{v}\int_0^\infty dx'\int d\mathbf{l}_\parallel^0\Theta(E_F-\varepsilon_0)\Theta(l_1^2-(l_\parallel^0)^2-\mathbf{Q}\cdot\mathbf{v})\times|m_{\varkappa\leftarrow\mathbf{l}_0}|^2, \quad (19)$$

and W_v is the interference term due to the vicinage effect,

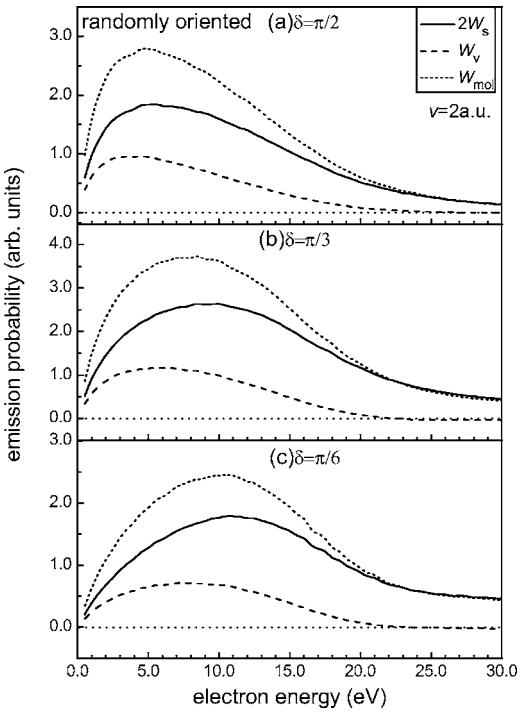

FIG. 5. Differential probability of electron emission vs electron energy, induced by N_2^+ ions grazingly scattered from a C surface at speed $v=2$ a.u., with the molecular axis randomly oriented. Results are shown for three electron emission angles relative to the surface, (a) $\delta=\pi/2$, (b) $\delta=\pi/3$, and (c) $\delta=\pi/6$.

$$W_v=\frac{8\pi}{v}\int_0^\infty dx'\int d\mathbf{l}_\parallel^0\Theta(E_F-\varepsilon_0)\Theta(l_1^2-(l_\parallel^0)^2-\mathbf{Q}\cdot\mathbf{v})\times|m_{\varkappa\leftarrow\mathbf{l}_0}|^2\cos\mathbf{Q}\cdot\mathbf{R}_0. \quad (20)$$

As before, for the case of a randomly oriented axis, one obtains the averaged expression for the vicinage term,

$$\bar{W}_v=\frac{8\pi}{v}\int_0^\infty dx'\int d\mathbf{l}_\parallel^0\Theta(E_F-\varepsilon_0)\Theta(l_1^2-(l_\parallel^0)^2-\mathbf{Q}\cdot\mathbf{v})\times|m_{\varkappa\leftarrow\mathbf{l}_0}|^2J_0(QR_0). \quad (21)$$

Figure 5 shows the integrated electron emission distributions as functions of the emitted electron energy for N_2^+ ions scattered from a C surface, with the incident angle $\theta=3$ mrad, the incident speed $v=2$, and a randomly oriented internuclear vector. Figures 5(a)–5(c) correspond to three different observation angles δ with respect to the surface plane. Most of the emitted electrons originate from the electron gas above the topmost atomic layer and are excited by the decay of the surface plasmon. Thus the energy spectra from individual ions exhibit broad maxima around $\omega_s-\Phi\approx11.2$ eV (where $\Phi\approx0.165$) in directions close to the surface, say with $\delta=\pi/6$, whereas the peaks occur at lower energies for observation angle $\delta=\pi/2$, indicating a mixing of the plasmon decay and the single-electron excitation mechanisms. One can also see from all three parts of Fig. 5 that the vicinage parts of the electron emission have their peak positions located at lower energies compared to the spectra of the iso-

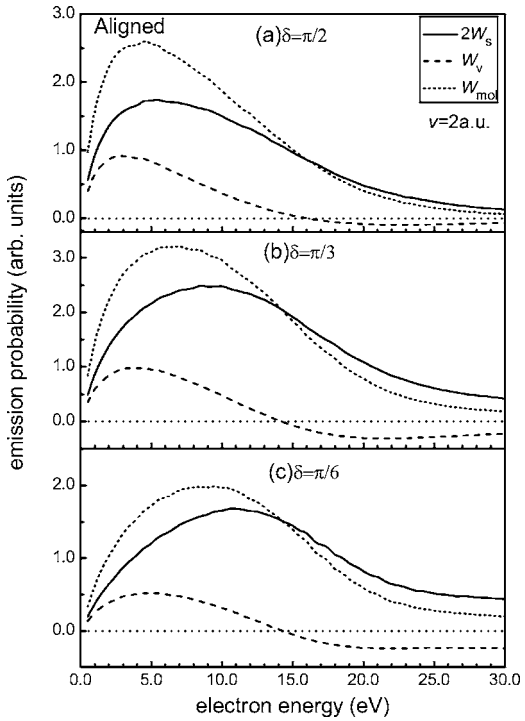

FIG. 6. Differential probability of electron emission vs electron energy, induced by N_2^+ ions grazingly scattered from a C surface at speed $v=2$ a.u., with the molecular axis aligned in the beam direction. Results are shown for three electron emission angles relative to the surface, (a) $\delta=\pi/2$, (b) $\delta=\pi/3$, and (c) $\delta=\pi/6$.

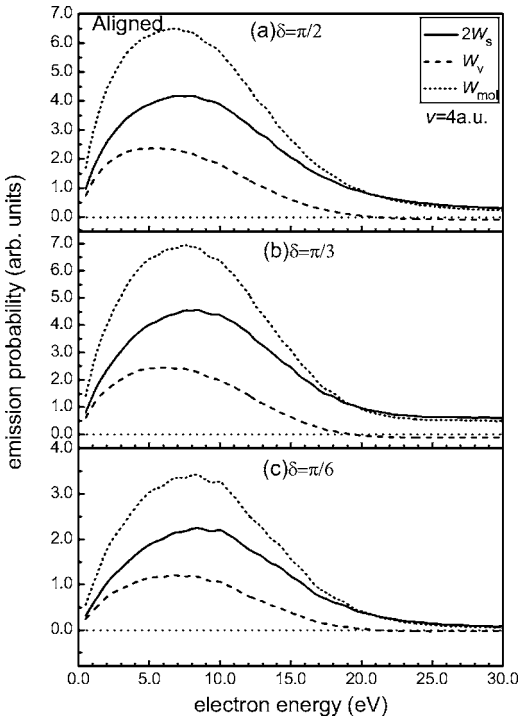

FIG. 7. Differential probability of electron emission vs electron energy, induced by N_2^+ ions grazingly scattered from a C surface at speed $v=4$ a.u., with the molecular axis aligned in the beam direction. Results are shown for three electron emission angles relative to the surface, (a) $\delta=\pi/2$, (b) $\delta=\pi/3$, and (c) $\delta=\pi/6$.

lated ions, suggesting a possibly more important role played by the single-electron excitations in the vicinage effect, which result in shifting of the peaks in the total electron emission spectra to lower energies.

Figure 6 shows how negative vicinage effect arises in the energy spectra of the electron emission for ion speed $v=2$ in the case of the aligned axis, while no trace of this kind of effect can be found in Fig. 7 where the incident speed is higher. As one can see from the comparison of Figs. 4 and 6, the decrease in the total energy loss for aligned internuclear axis is accompanied by a decrease in the number of electrons emitted at higher energies, while more electrons with lower energies are excited and emitted, especially at the observation angles $\delta=\pi/3$ and $\pi/6$. Thus, as a result of the vicinage effect, the electron emission spectra are shifted to lower energies, while the long tails of these spectra in the high-energy region disappear.

VI. SUMMARY

In this work, vicinage effects in the energy loss and the energy spectra of the emitted electrons have been discussed for grazing scattering of swift N_2^+ ions from a C solid surface. Using the dielectric response theory and the specular reflection model, we have formulated the equations of motion for the molecule center of mass and for the relative motion of the two constituent ions. Hence the molecule scattering trajectory and its Coulomb explosion dynamics were resolved in a consistent manner, for both the case of the molecular axis aligned in the direction of motion of the molecule, and the case of the axis randomly oriented in a plane parallel to the surface. The vicinage effect on the energy loss has been evaluated by means of the position-dependent stopping power, as a function of the incident angle, the incident speed, and the internuclear distance. The energy spectra of the emitted electrons have been obtained on the basis of the first-order, time-dependent perturbation theory, upon integration along the classical trajectory of the molecule.

Our calculations indicate that the vicinage effect in the energy loss is generally weaker for heavier molecules during grazing scattered from a solid surface, owing to the partial stripping of the constituent ions, although the absolute energy losses may be greater than those of light ions. In addition, while we have always obtained positive vicinage effect in the energy losses for molecules with randomly oriented axes, the cases of a molecular axis aligned in the direction of motion were found to exhibit negative vicinage effect in the energy losses especially at lower projectile speeds. Similar conclusions were derived for molecular penetration through solid foils. Thus a negative vicinage effect in the energy loss during grazing scattering may provide reasonable evidence that the internuclear vector was aligned with the beam velocity during the interaction with the surface.

Finally, a similar kind of the negative vicinage effect has been also found in the energy spectra of the emitted electrons, induced by slower molecules with the axis aligned in the direction of motion. In particular, the interference parts of

the emitted electron distributions exhibit in such cases a reduction in the electron emission at high energies, accompanied by an increase in the emission at low energies. Thus one can conclude that, generally, the negative vicinage effects in both the projectile energy losses and the emitted electron energy spectra during grazing scattering of heavy diatomic molecules from solid surfaces are caused by three factors: partial stripping of the constituent ions, low projectile speed, and the alignment of the molecular axis in the beam direction.

ACKNOWLEDGMENTS

This work was supported by the National Natural Science Foundation of China (Y.N.W., Grant No. 10275009). Z.L.M. acknowledges support by NSERC and PREA.

[1] Y. Susuki, H. Mukai, K. Kimura, and M. Mannami, Nucl. Instrum. Methods Phys. Res. B **48**, 347 (1990).
[2] H. Winter, J. C. Poizat, and J. Remillieux, Nucl. Instrum. Methods Phys. Res. B **67**, 345 (1992).
[3] Y. Susuki, T. Ito, K. Kimura, and M. Mannami, J. Phys. Soc. Jpn. **61**, 3535 (1992).
[4] Y. Susuki, T. Ito, K. Kimura, and M. Mannami, Phys. Rev. A **51**, 528 (1995).
[5] W. Brandt, A. Tatkowsky, and R. H. Ritchie, Phys. Rev. Lett. **33**, 1325 (1974).
[6] N. R. Arista, Nucl. Instrum. Methods Phys. Res. B **164–165**, 108 (2000).
[7] J. Jensen and P. Sigmund, Phys. Rev. A **61**, 032903 (2000).
[8] Y. Susuki, Phys. Rev. A **56**, 2918 (1997).
[9] Y. N. Wang, Z. L. Mišković, and W. K. Liu, Phys. Rev. A **58**, 1287 (1998).
[10] M. F. Steuer, D. S. Gemmell, E. P. Kanter, E. A. Johnson, and B. J. Zabransky, Nucl. Instrum. Methods Phys. Res. **194**, 277 (1982).
[11] Z. L. Mišković, S. G. Davison, F. O. Goodman, W. K. Liu, and Y. N. Wang, Phys. Rev. A **63**, 022901 (2001).
[12] H. W. Li, Y. N. Wang, and Z. L. Mišković, Nucl. Instrum. Methods Phys. Res. B **193**, 204 (2002).
[13] H. Winter, Phys. Rep. **367**, 387 (2002).
[14] H. Winter and H. P. Winter, Europhys. Lett. **62**, 739 (2003).
[15] S. Lederer, K. Maass, D. Blauth, H. Winter, H. P. Winter, and F. Aumayr, Phys. Rev. B **67**, 121405(R) (2003).
[16] F. J. García de Abajo and P. M. Echenique, Nucl. Instrum. Methods Phys. Res. B **79**, 15 (1993).
[17] Y. H. Song, Y. N. Wang, and Z. L. Miskovic, Phys. Rev. A **68**, 022903 (2003).
[18] M. N. Faraggi, M. S. Gravielle, and V. M. Silkin, Phys. Rev. A **69**, 042901 (2004).
[19] Y. H. Song, Y. N. Wang, and Z. L. Miskovic, Phys. Rev. A **63**, 052902 (2001).
[20] M. S. Gravielle, J. E. Miraglia, G. G. Otero, E. A. Sánchez, and O. Grizzi, Phys. Rev. A **69**, 042902 (2004).
[21] Y. Susuki, Z. Phys. D: At., Mol. Clusters **42**, 293 (1997).
[22] Y. H. Song and Y. N. Wang, Nucl. Instrum. Methods Phys. Res. B **153**, 186 (1999).
[23] W. Brandt and M. Kitagawa, Phys. Rev. B **25**, 5631 (1982).
[24] Y. N. Wang, Y. H. Song, Z. L. Miskovic, and W. K. Liu, Nucl. Instrum. Methods Phys. Res. B **153**, 26 (1999).
[25] F. J. García de Abajo and P. M. Echenique, Phys. Rev. B **46**, 2663 (1992).
[26] R. Garcia-Molina and S. Heredia-Avalos, Phys. Rev. A **63**, 044901 (2001).
[27] J. F. Ziegler, J. P. Biersack, and U. Littmark, *The Stopping and Ranges of Ions in Matter* (Pergamon, Oxford, 1985), Vol. 1.
[28] H. Bethe and Edwin Salpeter, *Quantum Mechanics of One and Two-Electron Atoms* (Springer-Verlag, Berlin, 1957).
[29] R. E. Wilems, Ph.D. thesis, University of Tennessee, 1968 (unpublished).